nature plants

Letter

https://doi.org/10.1038/s41477-023-01521-x

Systemic movement of long non-coding RNA *ELENA1* attenuates leaf senescence under nitrogen deficiency

Received: 16 November 2022

Accepted: 21 August 2023

Published online: 21 September 2023

Check for updates

Steven Le Hung Cheng[1,2], Haiying Xu[1], Janelle Hui Ting Ng[1] & Nam-Hai Chua[1,3,4]

Nitrogen is an essential macronutrient that is absorbed by roots and stored in leaves, mainly as ribulose-1,5-bisphosphate carboxylase/oxygenase[1,2]. During nitrogen deficiency (−N), plants activate leaf senescence for source-to-sink nitrogen remobilization for adaptative growth[3–6]. However, how −N signals perceived by roots are propagated to shoots remains underexplored. We found that *ELF18-INDUCED LONG NONCODING RNA 1* (*ELENA1*) is −N inducible and attenuates −N-induced leaf senescence in *Arabidopsis*. Analysis of plants expressing the *ELENA1* promoter β-glucuronidase fusion gene showed that *ELENA1* is transcribed specifically in roots under −N. Reciprocal grafting of the wild type and *elena1* demonstrated that *ELENA1* functions systemically. *ELENA1* dissociates the MEDIATOR SUBUNIT 19a–ORESARA1 transcriptional complex, thereby calibrating senescence progression. Our observations establish the systemic regulation of leaf senescence by a root-derived long non-coding RNA under −N in *Arabidopsis*.

Nitrogen is one of three essential macronutrients for plant growth[1]. In soil, nitrogen is available mainly in the form of nitrate ions[1], which are taken up by nitrate transporters expressed in roots. Nitrate ions can be transported to shoots and assimilated into various essential biological molecules such as DNA, RNA and proteins[1,2,7]. A major part of the nitrogen content in plants is stored as ribulose-1,5-bisphosphate carboxylase/oxygenase (RUBISCO) in leaves[2].

During nitrogen deficiency (−N), the master transcription factor of plant senescence *ORESARA1* (*ORE1*) is expressed. Together with MEDIATOR SUBUNIT 19a (MED19a)[3], ORE1 activates the transcription of several senescence-associated genes such as *BIFUNCTIONAL NUCLEASE 1* (*BFN1*), *RIBONUCLEASE 3* (*RNS3*), *SENESCENCE ASSOCIATED GENE 29* (*SAG29*), *SEVEN-IN-ABSENTIA 1* (*SINA1*) and *VND-INTERACTING 2* (*VNI2*) in leaves[4–6,8–10]. Enzymes encoded by these *ORE1* target genes are responsible for the degradation of nitrogen-rich molecules in mature leaves for the redistribution of nitrogen-containing metabolites to nitrogen-demanding organs in a source-to-sink manner[4–6].

However, how signals perceived by roots are used to systemically regulate leaf senescence during −N-adaptive growth remains underexplored. Here we show that the MED19a-associated[11] long non-coding RNA (lncRNA) *ELF18-INDUCED LONG NONCODING RNA 1* (*ELENA1*) transcripts are mobile and can move from roots to shoots to calibrate the rate of *ORE1*-dependent leaf senescence under −N by dissociating the MED19a–ORE1 transcription complex.

To examine the inducibility of *ELENA1* under −N, a time-course assay of wild-type (WT) seedlings grown on nitrogen-sufficient (+N) and −N media was performed, and RNAs from shoots and roots were extracted. Figure 1a shows that *ELENA1* transcripts were induced in a time-dependent manner under −N, beginning from day 2 of −N treatment, and accumulated in shoots up to about 400-fold on day

[1]Temasek Life Sciences Laboratory, National University of Singapore, Singapore, Singapore. [2]Department of Biological Sciences, National University of Singapore, Singapore, Singapore. [3]Department of Biochemistry, School of Medicine, National University of Singapore, Singapore, Singapore. [4]Disruptive & Sustainable Technologies for Agricultural Precision, Singapore–MIT Alliance for Research and Technology, Singapore, Singapore. e-mail: chua@rockefeller.edu

https://doi.org/10.1038/s41477-023-01521-x

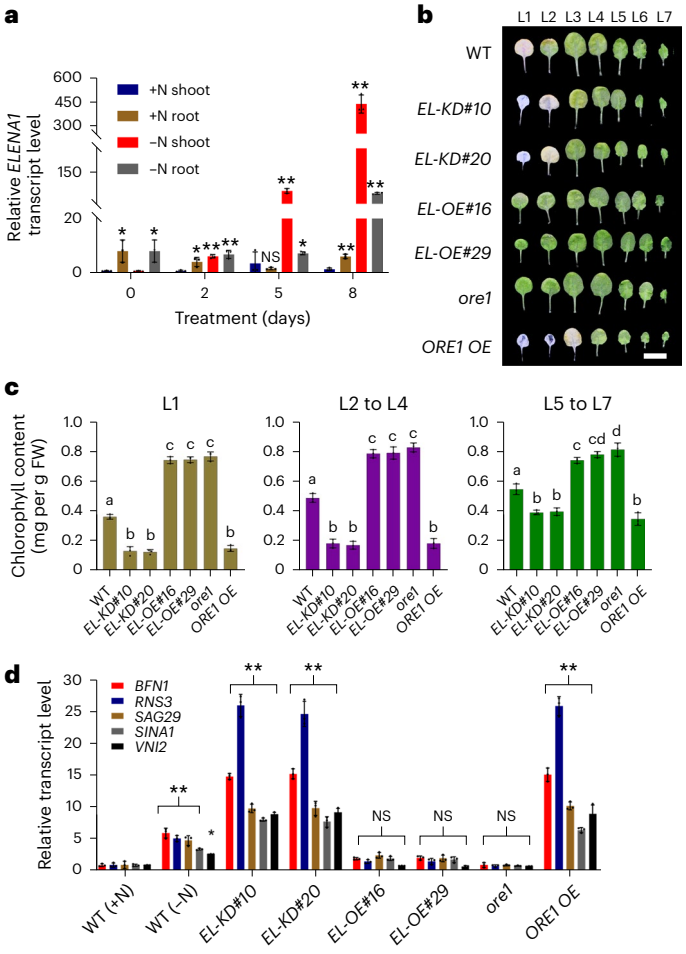

Fig. 1 | Long non-coding RNA *ELENA1* attenuates senescence induced by −N. **a**, Quantitative RT–PCR (RT–qPCR) analysis of *ELENA1* transcripts in shoots and roots of WT plants under +N and −N conditions at the indicated time after treatments. The value of +N shoots at day 0 was set as 1. The data are shown as means ± s.d. $n = 3$ (biologically independent samples). Each sample contained 20 seedlings, and individual data points are shown as overlays. The asterisks indicate statistically significant differences. $^{*}P < 0.05$; $^{**}P < 0.01$ (one-way analysis of variance (ANOVA), Dunnett's multiple comparison analysis). **b**, −N-induced leaf senescence phenotype of 17-day-old *Arabidopsis* plants of the indicated genotypes treated on −N medium for 17 days. Scale bar, 1 cm. **c**, Total chlorophyll content in different leaf groups of the indicated genotypes treated on −N medium. The letters indicate groups with statistically significant differences ($P < 0.05$, one-way ANOVA, Tukey's multiple comparison analysis). L, leaf number; FW, fresh weight. **d**, Transcript analysis of *ORE1* target genes *BFN1*, *RNS3*, *SAG29*, *SINA1* and *VNI2* in the indicated genotypes treated on +N or −N medium. The expression of each gene in the WT (+N) was set to 1. The data are shown as means ± s.d. $n = 3$ (biologically independent samples). Each sample contained 20 seedlings, and individual data points are shown as overlays. The asterisks indicate statistically significant differences compared with the WT (+N). $^{*}P < 0.05$; $^{**}P < 0.01$ (two-way ANOVA, Dunnett's multiple comparison analysis).

8 compared with day 0. By contrast, root *ELENA1* transcript levels increased to about 60-fold in day 8 roots relative to day 0. The differential accumulation of *ELENA1* transcripts in shoots compared with roots suggests that *ELENA1* may play a regulatory role in the adaptive developmental processes of shoots under −N, one of which is −N-induced leaf senescence.

To investigate the function of *ELENA1* under −N in shoots, we performed −N-induced leaf senescence assays using *ELENA1* knockdown (KD) and overexpressing (OE) plants described previously and compared their phenotypes against the well-characterized controls, *ore1* and *ORE1 OE*[11]. *ELENA1* KD plants (*EL-KD#10* and *EL-KD#20*) and *ELENA1* OE plants (*EL-OE#16* and *EL-OE#29*) displayed accelerated and delayed leaf senescence phenotypes, respectively, when compared with the WT (Fig. 1b,c). The phenotypes of EL-KD and EL-OE were antiparallel with those of *ore1* and *ORE1 OE*, respectively, and correlated with *ELENA1* levels in the mentioned genotypes (Fig. 1b,c and Extended Data Fig. 1). Transcript levels of *ORE1* target genes (*BFN1*, *RNS3*, *SAG29*, *SINA1* and *VNI2*) were monitored under −N. *EL-KD#10* and *EL-KD#20* exhibited enhanced expression of *ORE1* target genes, whereas *EL-OE#16* and *EL-OE#29* plants showed reduced expression compared with the WT under −N conditions (Fig. 1d). The changes in transcript levels (Fig. 1d) are consistent with the phenotypic observations (Fig. 1b,c) suggesting that *ELENA1* could be a negative regulator of *ORE1*-dependent −N-induced leaf senescence. *ELENA1* transcript levels in the WT (−N), *ore1* and *ORE1 OE* were comparable (Extended Data Fig. 1). Furthermore, using *ORE1–HA OE* plants, we found that ORE1 was not enriched on the genomic region upstream of the *ELENA1* transcriptional start site (TSS) under −N compared with +N (Supplementary Fig. 1). Together, these results suggest that *ELENA1* is not a downstream target of *ORE1* and is expressed in parallel with *ORE1* (Fig. 1a, Extended Data Fig. 1 and Supplementary Fig. 1)

To investigate whether *ELENA1* influences plant growth under +N conditions, we analysed chlorophyll content, plant morphology, fresh weight, nitrate content and the expression of *ORE1* target genes in the WT, *EL-KD#10* and *EL-OE#16* (Extended Data Fig. 2 and Supplementary Figs. 2 and 3) grown on +N medium. Total chlorophyll content, fresh weight and nitrate content were similar among the WT, *EL-KD#10* and *EL-OE#16*, suggesting that *ELENA1* probably does not influence nitrate uptake, assimilation or accumulation under +N condition (Extended Data Fig. 2a,b and Supplementary Fig. 2). Furthermore, fresh weight and nitrate content between shoots and roots of the WT, *EL-KD#10* and *EL-OE#16* were similar, demonstrating that *ELENA1* does not influence biomass and nitrate distribution under +N conditions (Extended Data Fig. 2b,d). These results (Extended Data Fig. 2 and Supplementary Figs. 2 and 3) rule out the possibility that the accelerated and delayed senescence of EL-KD and EL-OE, respectively, compared with the WT (Fig. 1b) was due to differing endogenous nitrate content prior to −N treatment. Furthermore, the expression of ORE1 target genes under +N remained relatively similar among the genotypes (Extended Data Fig. 2e), and the observation of similar growth morphology between the WT, *EL-KD#10* and *EL-OE#16* suggests that *ELENA1* does not influence normal plant growth under +N conditions (Extended Data Fig. 2e and Supplementary Fig. 3).

Several lncRNAs have been found to contain short open reading frames that encode functional peptides[12–14]. The *ELENA1* transcript contains eight ATGs and five open reading frames encoding putative peptides between 12 and 43 amino acids long[11]. We expressed *ELENA1* mutants with five or eight ATG mutations (EL^{5M}-OE and EL^{8M}-OE) as described previously[11] and assayed plants with comparable *ELENA1* expression levels to that of *EL-OE#16*, under −N (Extended Data Fig. 3a). We found that the EL^{5M}-OE and EL^{8M}-OE mutants had a comparable delayed senescence phenotype to that of EL-OE#16 when compared with WT empty-vector plants (Extended Data Fig. 3). These results suggest that the senescence-related function of *ELENA1* does not involve any encoded peptides and that *ELENA1* functions as a bona fide lncRNA under −N.

Under −N, leaf senescence progresses in the order of chronological leaf age for the remobilization of nitrogen from old to young leaves[8,9]. It is possible that *ELENA1* could act spatiotemporally in the shoot. Analysis of individual WT leaves, in chronological leaf age order, showed that *ELENA1* transcripts were differentially accumulated in younger, non-senescent leaves, following the duration of −N treatment (Extended Data Fig. 4). By contrast, *ORE1* transcript levels were relatively similar in the various leaves throughout −N treatment. This result corroborates the earlier observation that *ELENA1* is a negative regulator of −N-induced leaf senescence and suggests that *ELENA1* transcripts negatively regulate ORE1 function (Extended Data Fig. 4).

https://doi.org/10.1038/s41477-023-01521-x

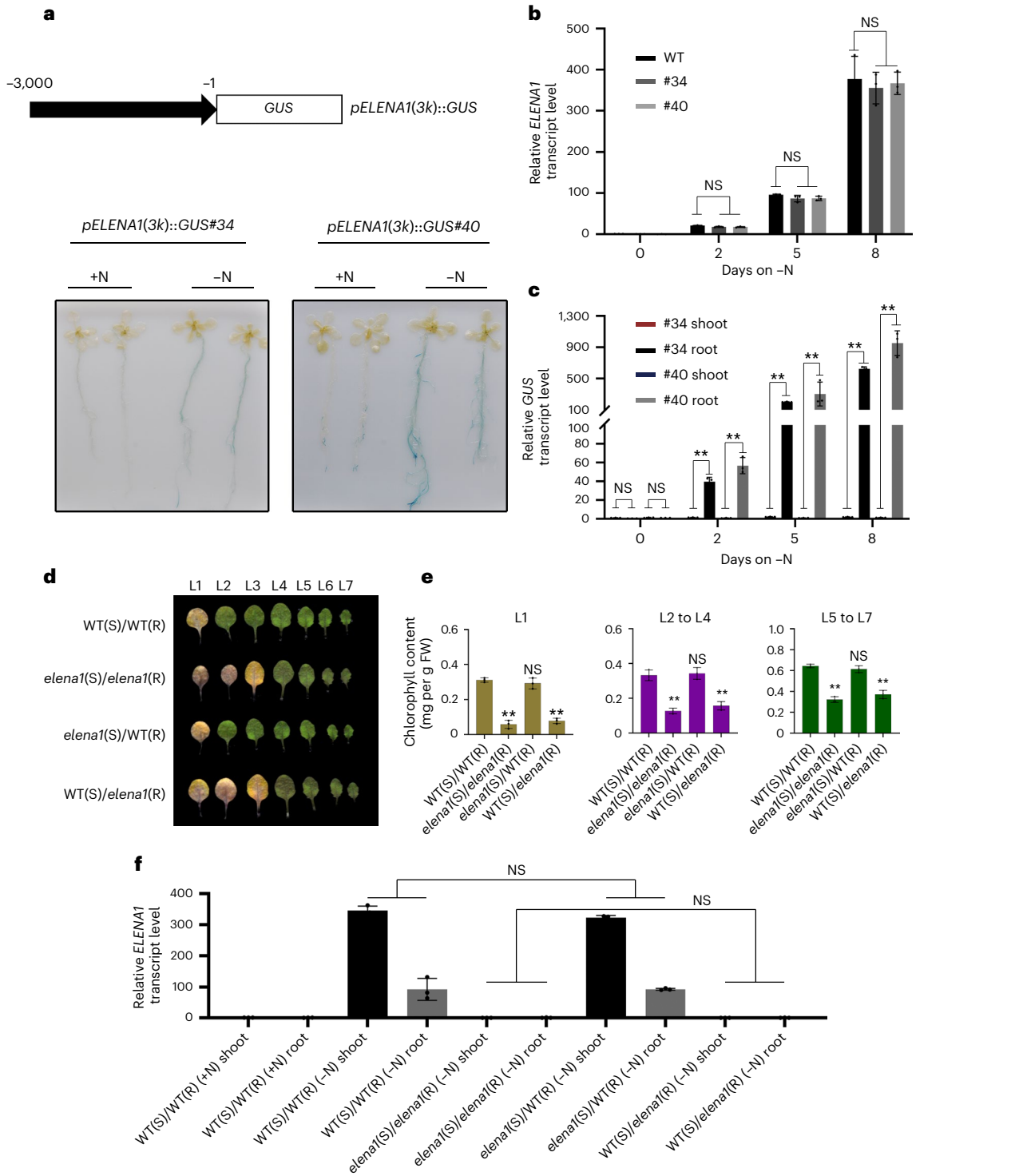

Fig. 2 | *ELENA1* is a root-to-shoot signalling molecule under −N conditions. **a**, GUS reporter assay of *ELENA1* promoter activity under +N and −N conditions. Top, schematic of *pELENA1(3k)*::*GUS* construct. The solid arrow indicates the genomic region upstream of *ELENA1*, and the numbers represent bp upstream of the *ELENA1* TSS. Bottom, representative GUS activity of the indicated transgenic lines expressing GUS treated on +N and −N media for ten days and incubated with GUS staining solution overnight. **b**, Determination of *ELENA1* transcript levels in the WT, *pELENA1(3k)*::*GUS #34* and *pELENA1(3k)*::*GUS #40* treated for zero, two, five and eight days in −N conditions. The value for the WT at day 0 was set as 1. **c**, Determination of *GUS* transcript levels in *pELENA1(3k)*::*GUS #34* and *pELENA1(3k)*::*GUS #40* treated for zero, two, five and eight days in −N conditions. RNA was extracted from shoots and roots. The value for line #34 shoots at day 0 was set as 1. **d**, −N-induced leaf senescence phenotype of 21-day-old WT and *elena1* graft chimeras treated on −N medium for 17 days. **e**, Total chlorophyll content in different leaf groups of the indicated graft chimeras treated on −N medium. The value for the WT(S)/WT(R) +N shoot was set to 1. **f**, Quantification of *ELENA1* transcript levels in the shoots and roots of the indicated graft chimeras treated on +N or −N medium. In **b**,**c**,**e**,**f**, the data are shown as means ± s.d. $n = 3$ (biologically independent samples). Each sample contained 20 seedlings, and individual data points are shown as overlays. The asterisks indicate statistically significant differences. $^{**}P < 0.01$ (one-way ANOVA, Dunnett's multiple comparison analysis).

https://doi.org/10.1038/s41477-023-01521-x

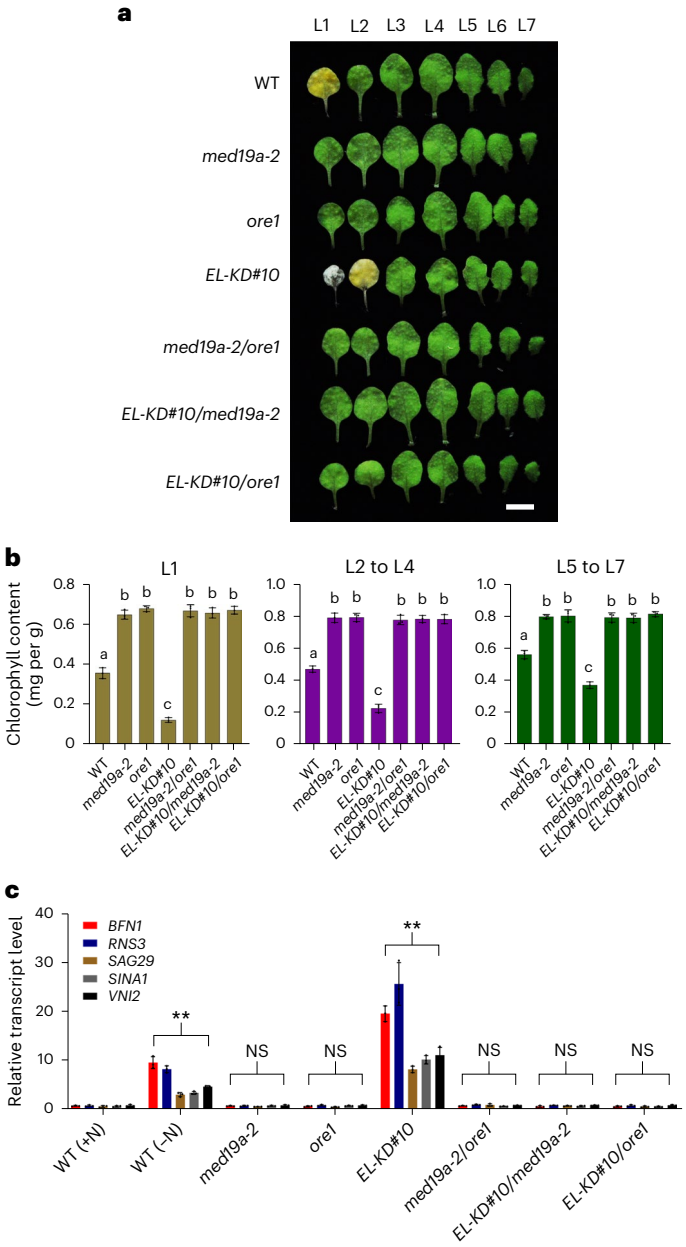

Fig. 3 | *ELENA1* genetically interacts with *MED19a* and *ORE1* under −N. **a**, −N-induced leaf senescence phenotype of 17-day-old *Arabidopsis* plants of the indicated genotypes treated on −N medium for 17 days. Scale bar, 1 cm. **b**, Total chlorophyll content in different leaf groups of the indicated genotypes treated on −N medium. The data are shown as means ± s.d. $n = 3$ (biologically independent samples). Each sample contained 20 seedlings, and individual data points are shown as overlays. The letters indicate groups with statistically significant differences ($P < 0.05$, one-way ANOVA, Tukey's multiple comparison analysis). **c**, RT–qPCR analysis of *ORE1* target genes *BFN1*, *RNS3*, *SAG29*, *SINA1* and *VNI2* in the indicated genotypes treated on +N or −N medium. The asterisks indicate statistically significant differences compared with the WT (+N). $^{**}P < 0.01$ (two-way ANOVA, Dunnett's multiple comparison analysis). The expression of each gene in the WT (+N) was set to 1. The data are shown as means ± s.d. $n = 3$ (biologically independent samples). Each sample contained 20 seedlings, and individual data points are shown as overlays.

The differential accumulation of *ELENA1* in shoots and roots raises the physiological issue of the site of *ELENA1* transcription under −N. To this end, we produced transgenic plants harbouring an *ELENA1* promoter–(3 kbp)-β-glucuronidase (GUS) fusion gene, and two independent homozygous lines, *pELENA1(3k)*::*GUS #34* and *#40*, were analysed (Fig. 2a and Supplementary Fig. 4). GUS staining under +N and −N treatment showed that the *ELENA1* promoter was active in roots but not shoots under −N (Fig. 2a). Furthermore, *ELENA1* levels in lines *#34* and *#40* were similar to that of the WT under −N (Fig. 2b). By contrast, *GUS* transcripts were found to be induced only in roots but not in shoots of these two lines under −N (Fig. 2c).

To determine the systemic function of *ELENA1* transcripts under −N, we generated an *elena1* CAS9 knockout allele that contained a deletion in the genomic region −297 to −7 base pairs (bp) upstream of the TSS using the promoter YAO CRISPR–CAS9 technology[15]. Plants homozygous for the *elena1* allele did not express *ELENA1* transcripts under −N, unlike the WT (Extended Data Fig. 5), demonstrating that *elena1* is a null allele under −N. Reciprocal graft chimeras of the WT and *elena1* were generated: WT scion (S) with WT rootstock (R) (WT(S)/WT(R)), *elena1*(S)/*elena1*(R), *elena1*(S)/WT(R) and WT(S)/*elena1*(R). These graft chimeras were assayed on −N for phenotypes and transcript levels (Fig. 2d,e). The WT(S)/WT(R) graft chimera displayed the −N-induced leaf senescence phenotype, whereas *elena1*(S)/*elena1*(R) displayed an accelerated senescence phenotype, consistent with the phenotypes of WT and EL-KD plants (Fig. 1a,b). Furthermore, *elena1*(S)/WT(R) exhibited −N-induced leaf senescence comparable to that of WT(S)/WT(R) (Fig. 2d,e), whereas WT(S)/*elena1*(R) displayed accelerated senescence comparable to that of *elena1*(S)/*elena1*(R) (Fig. 2d,e). Moreover, *ELENA1* transcript analysis in shoots and roots of the reciprocal graft chimeras demonstrated that WT rootstock was necessary for the normal expression of *ELENA1* transcripts, and the use of *elena1* rootstock was sufficient to completely suppress *ELENA1* transcript expression in the reciprocal graft chimeras (Fig. 2f). Transcript analysis of *ORE1* target genes under −N in shoots of the reciprocal graft chimeras showed that the presence of WT(R), in either WT(S)/WT(R) or *elena1*(S)/WT(R), was sufficient to activate *ORE1* target genes at normal levels under −N (Extended Data Fig. 6). By contrast, WT(S)/*elena1*(R) and *elena1*(S)/*elena1*(R) had elevated expression of *ORE1* target genes under −N (Extended Data Fig. 6). These results (Fig. 2 and Extended Data Fig. 6) show that *ELENA1* transcripts are transcribed in roots and act systemically in shoots to negatively regulate *ORE1*-dependent senescence under −N.

To provide additional evidence of the systemic root-to-shoot mobility of *ELENA1* transcripts, we generated WT(S)/WT(R) and WT(S)/EL-OE(R) graft chimeras. The presence of transgenic *ELENA1* transcripts in WT scions was detected by PCR using a primer pair that specifically amplifies transgenic *ELENA1* transcripts that contain the 35S 3′ sequences (Extended Data Fig. 7a). The specific 200-bp PCR amplicon was detected in PCR with reverse transcription (RT–PCR) of WT(S)/EL-OE(R) shoots but not in the reaction of WT(S)/WT(R) shoots (Extended Data Fig. 7a). Sequencing of these 200-bp PCR amplicons confirmed that these fragments were *ELENA1* transcripts (Extended Data Fig. 7c). Furthermore, we showed that transgenic *ELENA1* transcripts were systemically mobile under +N (Supplementary Fig. 5), suggesting that *ELENA1* root-to-shoot mobility is regulated by transcript abundance (Supplementary Fig. 5). Together, these observations (Fig. 2, Extended Data Fig. 7 and Supplementary Fig. 5) demonstrate that *ELENA1* transcripts are expressed specifically in roots under −N and transported to shoots to attenuate −N-induced leaf senescence.

ELENA1 was previously reported to interact with various mediator subunits—namely, MED19a, MED26b and MED36a[11,16]. We also recently reported that ORE1 interacts with MED19a to form a MED19a–ORE1 transcriptional complex necessary for −N-induced leaf senescence[3]. To investigate the genetic relationship of *ELENA1*, *MED19a* and *ORE1*, we generated various genetic crosses with *EL-KD#10*, *med19a-2* and *ore1* to acquire *med19a/ore1*, *EL-KD#10/med19a-2* and *EL-KD#10/ore1*. We found that the accelerated senescence phenotype of *EL-KD#10* was completely abolished in *EL-KD#10/med19a-2* and *EL-KD#10/ore1* to a level comparable to that of *med19a-2*, *ore1* and *med19a-2/ore1* when compared with the WT (Fig. 3a,b). A comprehensive genetic

https://doi.org/10.1038/s41477-023-01521-x

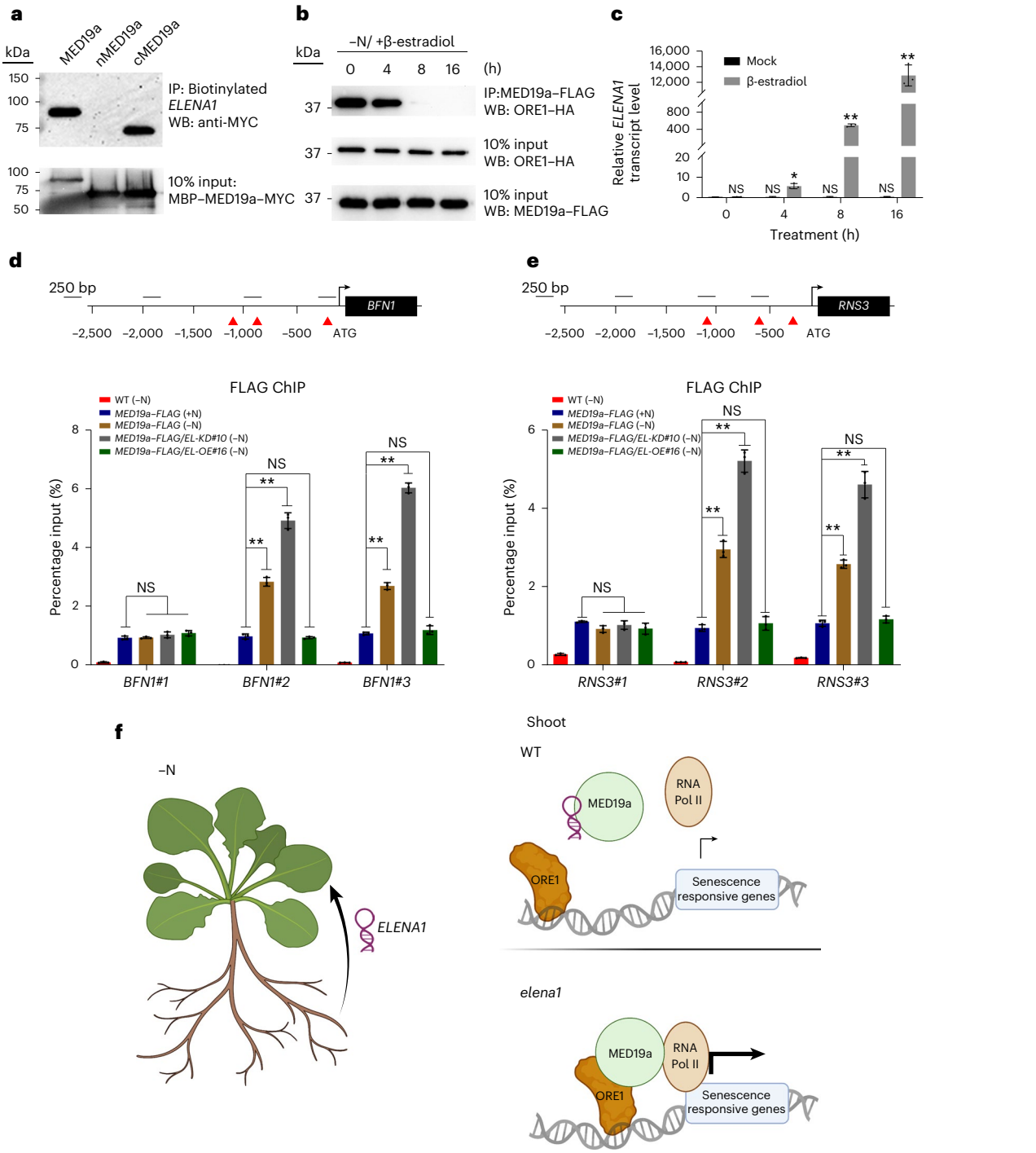

Fig. 4 | *ELENA1* dissociates the MED19a–ORE1 transcriptional complex. **a**, *ELENA1* interacts with the C-terminal region of MED19a in vitro. Top, RNA pull-down of biotinylated *ELENA1* transcripts against MED19a proteins detected by anti-MYC antibody. Bottom, 10% input of MBP–MED19a–MYC proteins and detected by western blot using anti-MYC antibody. **b**, In vivo interaction of MED19a and ORE1. *XVE::ELENA1/MED19a–FLAG OE/ORE1–HA OE* plants grown on –N medium were treated with β-estradiol for the indicated lengths of time. Top, immunoprecipitation of FLAG from the nuclear fraction followed by detection with HA antibody. Middle and bottom, 10% input of the nuclear fraction followed by detection with HA antibody and FLAG antibody, respectively. The experiment in **a**,**b** was repeated three times, with similar results. **c**, *XVE::ELENA1/MED19a–FLAG OE/ORE1–HA OE* plants grown on –N were treated without (mock) and with 50 μM β-estradiol, and *ELENA1* transcript levels were measured. The value under the mock treatment at time 0 was set to 1. **d**,**e**, Enrichment of MED19a–FLAG on the *BFN1* promoter (**d**) and on the *RNS3* promoter (**e**). WT, *MED19a–FLAG*, *MED19a–FLAG/EL-KD#10* and *MED19a–FLAG/EL-OE#16* plants were treated on +N or –N medium as indicated. The bars represent the means of percentage input of three biological repeats. The red triangles indicate putative binding sites for ORE1, and the black lines indicate probed regions. In **c**–**e**, the data are shown as means ± s.d. $n = 3$ (biologically independent samples). Each sample contained 20 seedlings, and individual data points are shown. The asterisks indicate statistically significant differences. $^{*}P < 0.05$; $^{**}P < 0.01$ (one-way ANOVA, Dunnett's multiple comparison analysis). **f**, Working model of *ELENA1* transcripts under –N. *ELENA1* is induced and transcribed in roots under –N, and the transcripts are transported systemically to shoots, where they are differentially accumulated in young leaves. *ELENA1* dissociates the MED19a–ORE1 complex, and the recruitment of RNA polymerase II (RNA Pol II) to target promoters is reduced, thereby attenuating the expression of ORE1 target genes to calibrate the rate of –N-induced leaf senescence. Image in **f** created with BioRender.com.

analysis of *ELENA1*, *MED19a* and *ORE1* further revealed that *ELENA1 OE* is sufficient to block the accelerated senescence phenotypes of *MED19a OE* and *ORE1 OE* (Extended Data Fig. 8). We also monitored *ORE1* and *MED19a* transcript levels and showed that they were comparable among the WT, *EL-KD#10* and *EL-KD#20* (Supplementary Fig. 6), suggesting that *ELENA1* transcripts do not regulate *MED19a* or *ORE1* expression. Transcript analysis showed that *ORE1* target genes were highly expressed in *EL-KD#10* compared with the WT (−N) (Fig. 3c). However, this increased expression was reduced in *EL-KD#10*/*med19a-2* and *EL-KD#10*/*ore1* to levels similar to those in the WT (+N) (Fig. 3c). These results (Fig. 3, Extended Data Fig. 8 and Supplementary Fig. 6) show that *Med19a* and *ORE1* are both needed for *ELENA1* to regulate −N-induced leaf senescence.

The genetic relationship of *ELENA1*, *MED19a* and *ORE1* raises the question of the possible effects of MED19a and ORE1 on the systemic root-to-shoot mobility of *ELENA1* transcripts under −N. We analysed *ELENA1* transcript levels in shoots and roots of WT, *med19a-2* and *ore1* plants treated on −N medium and found that *ELENA1* transcript levels in shoots and roots of the indicated genotypes remained relatively unchanged, suggesting that MED19a and ORE1 are probably not required for *ELENA1* root-to-shoot mobility (Extended Data Fig. 9).

To investigate the biochemical relationship between *ELENA1*, *MED19a* and *ORE1*, we performed an in vitro RNA pull-down assay. We found that the MED19a carboxy-terminal region but not the amino-terminal region, described previously[16], was necessary and sufficient to interact with biotinylated *ELENA1* transcripts (Fig. 4a). The MED19a C-terminal region was previously found to be necessary for ORE1 interaction[3]. This result raises the possibility that *ELENA1* transcripts could dissociate the MED19a–ORE1 complex by competing with ORE1 for the MED19a C-terminal region. An in vitro interaction assay of the MED19a–ORE1 protein complex with *ELENA1* transcripts was performed, and antisense *ELENA1* transcripts were used as a negative control (Extended Data Fig. 10). Extended Data Fig. 10 shows that *ELENA1* RNA, but not antisense *ELENA1* RNA, was sufficient to dissociate the MED19a–ORE1 complex. We performed in vivo immunoprecipitation experiments using *XVE*::*ELENA1*/*MED19a–FLAG OE*/*ORE1–HA OE* plants grown under −N and treated with β-estradiol inducer. We found that increasing *ELENA1* transcript levels were sufficient to dissociate the MED19a–ORE1 complex in vivo (Fig. 4b,c). Furthermore, MED19a and ORE1 form heterotypic condensates in vitro[3], which can be dissociated by *ELENA1* but not antisense *ELENA1* RNA (Supplementary Fig. 7).

To determine the function of *ELENA1* transcripts in MED19a enrichment on the genomic regions upstream of *BFN1* and *RNS3* under −N, we performed a chromatin immunoprecipitation (ChIP) assay of MED19a–FLAG (Fig. 4d,e). We previously reported that the enrichment of MED19a on the promoters of *BFN1* and *RNS3* is dependent on ORE1 and ORE1 binding sites. WT, *MED19a–FLAG OE*, *MED19a–FLAG OE*/*EL-KD#10* and *MED19a–FLAG OE*/*EL-OE#16* were treated under +N and −N conditions, and FLAG ChIP was performed (Fig. 4d,e). We found that enrichment levels of MED19a on *BFN1#2*, *BFN1#3*, *RNS#2* and *RNS#3* under −N were significantly elevated in *MED19a–FLAG OE*/*EL-KD#10* (−N) compared with *MED19a–FLAG OE* (−N) but reduced in *MED19a–FLAG OE*/*EL-OE#16* to levels similar to those in *MED19a–FLAG OE* (+N) (Fig. 4d,e). These results are consistent with the observation that *ELENA1* attenuates ORE1-dependent senescence under −N (Fig. 1) and that *ELENA1* transcripts are sufficient to dissociate the MED19a–ORE1 transcriptional complex (Fig. 4).

Systemically mobile RNAs have been found to harbour RNA structures and motifs such as tRNA-like structures[17] and polypyrimidine tracts that bind to polypyrimidine-binding proteins[18,19]. To determine whether *ELENA1* contains any of these features, we performed an in silico analysis of the secondary structure of *ELENA1* (Supplementary Fig. 8) using RNAfold[20]. The predicted minimal free energy and centroid RNA structures of *ELENA1* did not reveal a tRNA-like structure (Supplementary Fig. 8). The RNA sequence of *ELENA1* was analysed, and two regions with high polypyrimidine content were identified (Supplementary Fig. 9) and annotated as polypyrimidine tract 1 and 2 (PT1 and PT2). PT1 and PT2 contained higher pyrimidine (cytosine and uracil) content, 75% and 65%, respectively, than the 52% found in full-length *ELENA1*. The presence of PT1 and PT2 raises the possibility that polypyrimidine-binding proteins could facilitate the systemic mobility of *ELENA1* under −N conditions.

Like many transcription factors, ORE1 is regulated by post-translational modifications such as polyubiquitination[8], deubiquitination[9] and phosphorylation[21]. Our study shows the disruption of the MED19a–ORE1 transcriptional complex by lncRNA *ELENA1* transcripts under −N, thus adding another level of regulatory complexity. In addition, the tissue-specific expression of *ELENA1* under −N raises interesting questions on the role of this lncRNA in root development and the regulation of root nitrate transporters under −N conditions. In summary (Fig. 4d), we have shown that the −N-inducible *ELENA1* transcripts are transcribed in roots, are root-to-shoot mobile and are sufficient to dissociate the MED19a–ORE1 complex in leaves, thereby calibrating the progression of −N-induced leaf senescence. Future work should be directed towards understanding the mechanism of inter-organ movement of *ELENA1*.

Methods

Plant materials, preparation of constructs and transgenic plants, and growth conditions

Arabidopsis thaliana ecotype Columbia-0 was used as the WT. The *ELENA1* KD lines (*EL-KD#10* and *EL-KD#20*), *ELENA1* OE lines (*EL-OE#16* and *EL-OE#29*) and *ELENA1* mutant variant overexpressing lines (*ELENA1*_5M (EL^{5M}) and *ELENA1*_8M (EL^{8M})) have been described previously[11,16].

The mutants *med19a-2* (SALK_034955) and *ore1* (SALK_090154) were acquired from the Arabidopsis Biological Resource Centre. The *MED19a–FLAG* and *ORE1–HA OE* lines and *MED19a–FLAG OE*/*ORE1–HA OE* double expression lines have been described previously[3]. *EL-KD#10* was crossed with *med19a-2*, *MED19a–FLAG OE*, *ore1* and *ORE1–HA OE* to generate *EL-KD#10*/*med19a-2*, *EL-KD#10*/*MED19a OE*, *EL-KD#10*/*ore1* and *EL-KD#10*/*ORE1 OE*, respectively. *EL-OE#16* was crossed with *med19a-2*, *MED19a OE*, *ore1* and *ORE1 OE* to generate *EL-OE#16*/*med19a-2*, *EL-OE#16*/*MED19a OE*, *EL-OE#16*/*ore1* and *EL-OE#16*/*ORE1 OE*, respectively.

To generate the fusion of the *ELENA1* promoter and GUS, a DNA fragment 3 kbp upstream of *ELENA1* TSS was amplified by PCR and cloned into pDONR221 by BP reaction (Invitrogen) followed by LR reaction (Invitrogen) with pKGWFS7 (ref. 22) to obtain *pELENA1(3k)*::*GUS*. After sequence verification, the construct was transformed into *Agrobacterium* strain GV3101. *Agrobacterium*-mediated transformation by floral dipping[23] was performed on WT plants to obtain *pELENA1(3k)*::*GUS* transgenic plants. The lines were analysed for single insertion, and homozygous *pELENA1(3k)*::*GUS #34* and *pELENA1(3k)*::*GUS #40* lines were selected for experiments.

To generate the *elena1* Cas9 mutant, the *pYAO*-activated CRISPR–Cas9 system was utilized[15]. Guide RNAs targeting genomic regions flanking regions were designed with Benchling software. Successful CRISPR–Cas9 knockout was confirmed by PCR using flanking primers. Stable *elena1* mutant plants were obtained from the T_3 generation, and PCR amplicons obtained from PCR with genomic DNA were verified with DNA sequencing.

To generate the *XVE*::*ELENA1*/*MED19a OE*/*ORE1 OE* lines, *ELENA1* was cloned into pER8-DC[24] by LR cloning (Invitrogen) to obtain *XVE*::*ELENA1*. The *XVE*::*ELENA1* construct was verified by DNA sequencing and was transformed into *Agrobacterium* GV3101 followed by floral dipping[23] to generate *XVE*::*ELENA1*/*MED19a OE*/*ORE1 OE* seeds. The lines were analysed for single insertion and *ELENA1* inducibility with β-estradiol inducer treatment[24].

T_3 and T_4 homozygous seeds were obtained for experiments.

Plant growth conditions and −N treatment

Seeds on Murashige and Skoog (MS) medium without sucrose (−S) were stratified for at least two days, and the plates were placed vertically under 16 h/8 h light/dark conditions with 100 µmol m^{-2} s^{-1} light intensity. Seven-day-old seedlings were transferred to another MS medium (−S) for further propagation vertically for another ten days. The 17-day-old seedlings were transferred to phytatrays (Sigma) containing Hoagland's[8] hydroponics +N and −N medium with 1.2% Bactoagar.

+N and −N phenotypic observations and chlorophyll quantification

Seventeen-day-old *Arabidopsis* grown vertically on MS (−S) were treated on +N and −N media. The plants were observed 21 days post transfer to Hoagland's hydroponics +N or −N medium[8,9]. For chlorophyll quantification, leaves from −N-treated plants were separated into three groups in chronological developmental order: L1, L2–L4 and L5–L7. For plants treated on +N medium, the leaves were separated into four groups: L1, L2–L4, L5–L7, and L8 and L9.

The samples were pulverized with a mortar and pestle, and chlorophyll was extracted by incubating the powder with 80% ethanol overnight in 4 °C. The plant debris was pelleted by centrifugation at 21,000 *g*, and total chlorophyll was quantified by a 96-well plate reader (Tecan)[8,9].

Fresh weight and total nitrate content quantification

Fifteen-day-old seedlings propagated on MS medium (−S) were analysed. Shoots and roots derived from 20 seedlings were pooled separately to obtain the average fresh weight values of the two organs. The pools of plant tissues were pulverized with a mortar and pestle, and nitrate contents were determined using the salicylic–sulphuric acid colorimetric method[25].

RNA extraction, RT and qPCR

Plants grown on +N and −N media were pulverized with a mortar and pestle. Total RNAs were extracted using the Qiagen RNeasy plant mini kit with DNase treatment following the manufacturer's instructions. RNA concentrations were quantified using nanodrop and RT reactions with iScript (Bio-Rad) following the manufacturer's instructions. The cDNA generated was diluted appropriately. The qPCR reactions were prepared with cDNA, SyBR Green (Bio-Rad) and the appropriate qPCR primer pairs. The Bio-Rad CFX96 real-time system was used for qPCR measurement.

Plant grafting and *ELENA1* mobility assay

Five-day-old seedlings were used for grafting using transverse cut–butt grafting[26,27]. The seedlings were dissected at the hypocotyl with a razor blade to generate shoot and root. Chimeric combinations were generated according to experimental requirements. The graft chimeras were further propagated for another seven days. Successful graft chimeras were selected by physical examination under a bright field light microscope; the success rate was 50% to 80%. Adventitious roots were removed with a razor blade, and the plants were further propagated for an additional seven days. The 18- to 19-day-old seedlings were treated on +N/−N, and samples were harvested according to experimental requirements.

The *ELENA1* mobility assay was performed with WT/WT and WT/*UBQ10*::*ELENA1 OE* chimeras. Chimeric plants were treated on −N medium for 21 days, and root and shoot samples were harvested separately. RNA and genomic DNA were extracted according to a previous report[28]. RT–PCR, no RT–PCR, genomic DNA–PCR and ACTIN2 PCR were performed using Phusion polymerase for 35 cycles. PCR products were analysed on a 1.5% TAE agarose.

Heterologous recombinant protein expression and purification

MBP-tagged full-length MED19a, truncated nMED19a, cMED19a and GST-tagged ORE1 constructs were described previously[3].The expression constructs were transformed into *Escherichia coli* strain Rosetta, and expression clones were selected by appropriate antibiotics. The inducibility of the protein of interest was analysed by SDS–PAGE.

The protein expression and purification procedure was described previously[11]. Briefly, induced cells were lysed in lysis buffer and sonicated (Qsonica) on ice at 40% amplitude, 15 s on, 30 s off, 15 cycles. Cell lysates were centrifuged at 21,000 *g* for 1 h (Beckman Coulter). The supernatant was mixed with equilibrated amylose (NEB) or glutathione Sepharose 4B (GE healthcare) beads, and the manufacturers' instructions were followed to obtain purified proteins.

In vitro transcription of RNA

PCR was performed to generate DNA templates harbouring the T7 promoter upstream of the genes of interest (*ELENA1* and antisense *ELENA1*). Purified PCR fragments were added to the Megascript (Invitrogen) in vitro transcription (IVT) reaction and performed according to the manufacturer's instructions to generate label-free RNA. To generate biotin-labelled RNA, the IVT reaction NTP mix was replaced with biotin RNA labelling mix (Roche). RNA was purified with a Qiagen RNeasy mini kit and frozen at −80 °C for experiments.

In vitro protein, RNA pull-down assay and protein–RNA interaction assay

We incubated 1,000 ng of purified IVT biotinylated RNA with 500 ng of target protein in each tube in the RNA pull-down buffer. The bound proteins were washed three times with wash buffer (20 mM Tris HCl, 200 mM NaCl, 0.5% glycerol in DEPC treated H_2O)[11,16].

MBP–MED19a–MYC and GST–ORE1–HA proteins were preincubated for an hour in RNA pull-down buffer at room temperature to allow for complex formation. To test for the activity of IVT RNAs, *ELENA1* and antisense *ELENA1* were added in increasing amounts (0, 0.5, 1 and 2 µM) and incubated for an hour at room temperature. Equilibrated amylose (NEB) beads were added to each reaction tube and incubated for one hour. The beads were washed three times in wash buffer. The bound proteins were eluted by the addition of SDS–PAGE loading mix and analysed by 10% SDS–PAGE followed by western blotting with the appropriate antibodies. MYC tag antibody (Proteintech, 16286-1-AP) and HA tag antibody (Proteintech, 51064-2-AP) were used at 1:5,000 dilution.

In vitro condensate assay

The in vitro condensate assay[3] was performed by the addition of 10 µM cMED19a–mCherry to 1 µM ORE1–mECFP proteins in a reaction buffer containing 20 mM Tris pH 7.4, 200 mM NaCl and 10% (w/v) PEG 8000. *ELENA1* and antisense *ELENA1*, transcribed in vitro, were added in increasing amounts (0, 0.5, 1 and 2 µM) to the reaction mixture.

ChIP

Three grams of plant materials were harvested and crosslinked with formaldehyde. Isolated nuclei were sonicated to shear DNA[29,30]. Equilibrated FLAG-M2 (Sigma-Aldrich) beads were added to immunoprecipitate FLAG-tagged protein–DNA complex. Reverse crosslinking was performed, and DNA was purified using a DNA extraction kit (Qiagen). The percentage input of ChIP samples against 1% input was measured with qPCR (Bio-Rad).

β-estradiol treatment and nuclear in vivo co-IP

β-estradiol was dissolved in dimethyl sulfoxide. *XVE*::*ELENA1*/*UBQ10*::*MED19a–FLAG/35S*::*ORE1–HA* plants were grown on −N medium for 14 days. *XVE*::*ELENA1*/ *UBQ10*::*MED19a–FLAG/35S*::*ORE1–HA* plants were treated with 50 µM β-estradiol for 0, 4, 8 and 16 h. The nuclei were isolated[29], and equilibrated FLAG-M2 (Sigma-Aldrich) beads were added to bind MED19a–FLAG. The bound proteins were eluted by the addition of SDS–PAGE loading mix and analysed by western blotting with the

appropriate antibodies. MYC tag antibody (Proteintech, 16286-1-AP), HA tag antibody (Proteintech, 51064-2-AP) and FLAG tag antibody (Cell signalling, 9A3) were used at 1:5,000 dilution.

In silico RNA structure and sequence analysis

The RNA sequence of *ELENA1* was analysed with RNAfold[20] to obtain the predicted minimal free energy, centroid RNA secondary structures and the RNA secondary structure mountain plot. The *ELENA1* RNA sequence was visualized with Benchling.

Reporting summary

Further information on research design is available in the Nature Portfolio Reporting Summary linked to this article.

Data availability

All data generated or analysed in this study are included in this Letter and its Supplementary Information files. The materials and transgenic plants generated in this study are available from the corresponding author on reasonable request. Source data are provided with this paper.

References

1. Have, M. et al. Nitrogen remobilization during leaf senescence: lessons from *Arabidopsis* to crops. *J. Exp. Bot.* **68**, 2513–2529 (2017).
2. Feller, U., Anders, I. & Mae, T. Rubiscolytics: fate of Rubisco after its enzymatic function in a cell is terminated. *J. Exp. Bot.* **59**, 1615–1624 (2008).
3. Cheng, S. L. H. et al. Nutrient status regulates MED19a phase separation for ORESARA1-dependent senescence. *N. Phytol.* **236**, 1779–1795 (2022).
4. Balazadeh, S. et al. A gene regulatory network controlled by the NAC transcription factor ANAC092/AtNAC2/ORE1 during salt-promoted senescence. *Plant J.* **62**, 250–264 (2010).
5. Kim, J. H. et al. Trifurcate feed-forward regulation of age-dependent cell death involving miR164 in *Arabidopsis*. *Science* **323**, 1053–1057 (2009).
6. Rauf, M. et al. ORE1 balances leaf senescence against maintenance by antagonizing G2-like-mediated transcription. *EMBO Rep.* **14**, 382–388 (2013).
7. Diaz, C. et al. Nitrogen recycling and remobilization are differentially controlled by leaf senescence and development stage in *Arabidopsis* under low nitrogen nutrition. *Plant Physiol.* **147**, 1437–1449 (2008).
8. Park, B. S. et al. *Arabidopsis* NITROGEN LIMITATION ADAPTATION regulates ORE1 homeostasis during senescence induced by nitrogen deficiency. *Nat. Plants* **4**, 898–903 (2018).
9. Park, S. H. et al. *Arabidopsis* ubiquitin-specific proteases UBP12 and UBP13 shape ORE1 levels during leaf senescence induced by nitrogen deficiency. *N. Phytol.* **223**, 1447–1460 (2019).
10. Qiu, K. et al. EIN3 and ORE1 accelerate degreening during ethylene-mediated leaf senescence by directly activating chlorophyll catabolic genes in *Arabidopsis*. *PLoS Genet.* **11**, e1005399 (2015).
11. Seo, J. S. et al. ELF18-INDUCED LONG-NONCODING RNA associates with mediator to enhance expression of innate immune response genes in *Arabidopsis*. *Plant Cell* **29**, 1024–1038 (2017).
12. Liu, J., Wang, H. & Chua, N. H. Long noncoding RNA transcriptome of plants. *Plant Biotechnol. J.* **13**, 319–328 (2015).
13. Ma, L., Bajic, V. B. & Zhang, Z. On the classification of long non-coding RNAs. *RNA Biol.* **10**, 925–933 (2013).
14. Statello, L. et al. Gene regulation by long non-coding RNAs and its biological functions. *Nat. Rev. Mol. Cell Biol.* **22**, 96–118 (2021).
15. Yan, L. et al. High-efficiency genome editing in *Arabidopsis* using YAO promoter-driven CRISPR/Cas9 system. *Mol. Plant* **8**, 1820–1823 (2015).
16. Seo, J. S. et al. ELF18-INDUCED LONG NONCODING RNA 1 evicts fibrillarin from mediator subunit to enhance PATHOGENESIS-RELATED GENE 1 (PR1) expression. *N. Phytol.* **221**, 2067–2079 (2019).
17. Yang, L. et al. Heritable transgene-free genome editing in plants by grafting of wild-type shoots to transgenic donor rootstocks. *Nat. Biotechnol.* **41**, 958–967 (2023).
18. Liu, L. & Chen, X. Intercellular and systemic trafficking of RNAs in plants. *Nat. Plants* **4**, 869–878 (2018).
19. Ham, B. K. et al. A polypyrimidine tract binding protein, pumpkin RBP50, forms the basis of a phloem-mobile ribonucleoprotein complex. *Plant Cell* **21**, 197–215 (2009).
20. Gruber, A. R. et al. The Vienna RNA websuite. *Nucleic Acids Res.* **36**, W70–W74 (2008).
21. Durian, G. et al. Calcium-dependent protein kinase CPK1 controls cell death by in vivo phosphorylation of senescence master regulator ORE1. *Plant Cell* **32**, 1610–1625 (2020).
22. Karimi, M., Inze, D. & Depicker, A. GATEWAY vectors for *Agrobacterium*-mediated plant transformation. *Trends Plant Sci.* **7**, 193–195 (2002).
23. Zhang, X. et al. *Agrobacterium*-mediated transformation of *Arabidopsis thaliana* using the floral dip method. *Nat. Protoc.* **1**, 641–646 (2006).
24. Zuo, J., Niu, Q. W. & Chua, N. H. Technical advance: an estrogen receptor-based transactivator XVE mediates highly inducible gene expression in transgenic plants. *Plant J.* **24**, 265–273 (2000).
25. Huang, C. H. et al. Early diagnosis and management of nitrogen deficiency in plants utilizing Raman spectroscopy. *Front. Plant Sci.* **11**, 663 (2020).
26. Turnbull, C. G., Booker, J. P. & Leyser, H. M. Micrografting techniques for testing long-distance signalling in *Arabidopsis*. *Plant J.* **32**, 255–262 (2002).
27. Chen, X. et al. Shoot-to-root mobile transcription factor HY5 coordinates plant carbon and nitrogen acquisition. *Curr. Biol.* **26**, 640–646 (2016).
28. Edwards, K., Johnstone, C. & Thompson, C. A simple and rapid method for the preparation of plant genomic DNA for PCR analysis. *Nucleic Acids Res.* **19**, 1349 (1991).
29. Fiil, B. K. et al. Coimmunoprecipitation (co-IP) of nuclear proteins and chromatin immunoprecipitation (ChIP) from *Arabidopsis*. *CSH Protoc.* **2008**, pdb.prot5049 (2008).
30. Saleh, A., Alvarez-Venegas, R. & Avramova, Z. An efficient chromatin immunoprecipitation (ChIP) protocol for studying histone modifications in *Arabidopsis* plants. *Nat. Protoc.* **3**, 1018–1025 (2008).

Acknowledgements

We thank X. Qi for the gift of *pYAO* CRISPR–Cas9 vectors and C. Xiangbin for guidance on *Arabidopsis* grafting. This work was supported by core funding from Temasek Life Sciences Laboratory and Disruptive & Sustainable Technology for Agricultural Precision (DiSTAP), an interdisciplinary research group (IRG) of the Singapore MIT Alliance for Research and Technology (SMART) Centre supported by the National Research Foundation (NRF), Prime Minister's Office, Singapore, under its Campus for Research Excellence and Technological Enterprise (CREATE) programme.

Author contributions

S.L.H.C. and N.-H.C. designed the experiments. S.L.H.C., H.X. and J.H.T.N. executed the experiments. All the authors interpreted and discussed the data. S.L.H.C. and N.-H.C. wrote the paper.

Competing interests
The authors declare no competing interests.

Additional information
Extended data is available for this paper at https://doi.org/10.1038/s41477-023-01521-x.

Supplementary information The online version contains supplementary material available at https://doi.org/10.1038/s41477-023-01521-x.

Correspondence and requests for materials should be addressed to Nam-Hai Chua.

Peer review information *Nature Plants* thanks Yong Wang, Yasuhito Sakuraba, Martin Crespi and the other, anonymous, reviewer(s) for their contribution to the peer review of this work.

https://doi.org/10.1038/s41477-023-01521-x

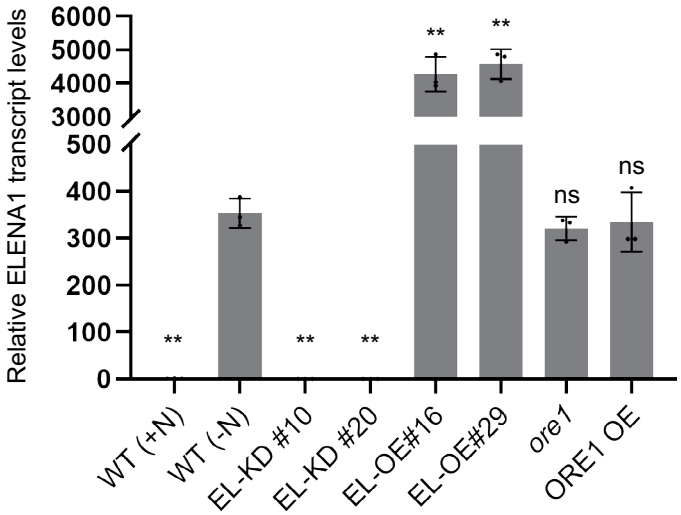

Extended Data Fig. 1 | *ELENA1* transcript levels in *ELENA1* and *ORE1* genotypes under nitrogen deficiency (-N). RT-qPCR analysis of *ELENA1* transcript levels in WT (Nitrogen sufficient; +N), WT (-N), *EL-KD#10*, *EL-KD#20*, *EL-OE#16*, *EL-OE#29*, *ore1* and *ORE1 OE* on -N. The value of WT (+ N) was set to 1. Data are means ± SD. n = 3 (biologically independent repeats) and individual data points as overlays. ns, no statistical difference. Asterisks indicate statistically significant difference compared with WT (-N). $^{**}P < 0.01$; one-way ANOVA, Dunnett's multiple comparison analysis.

https://doi.org/10.1038/s41477-023-01521-x

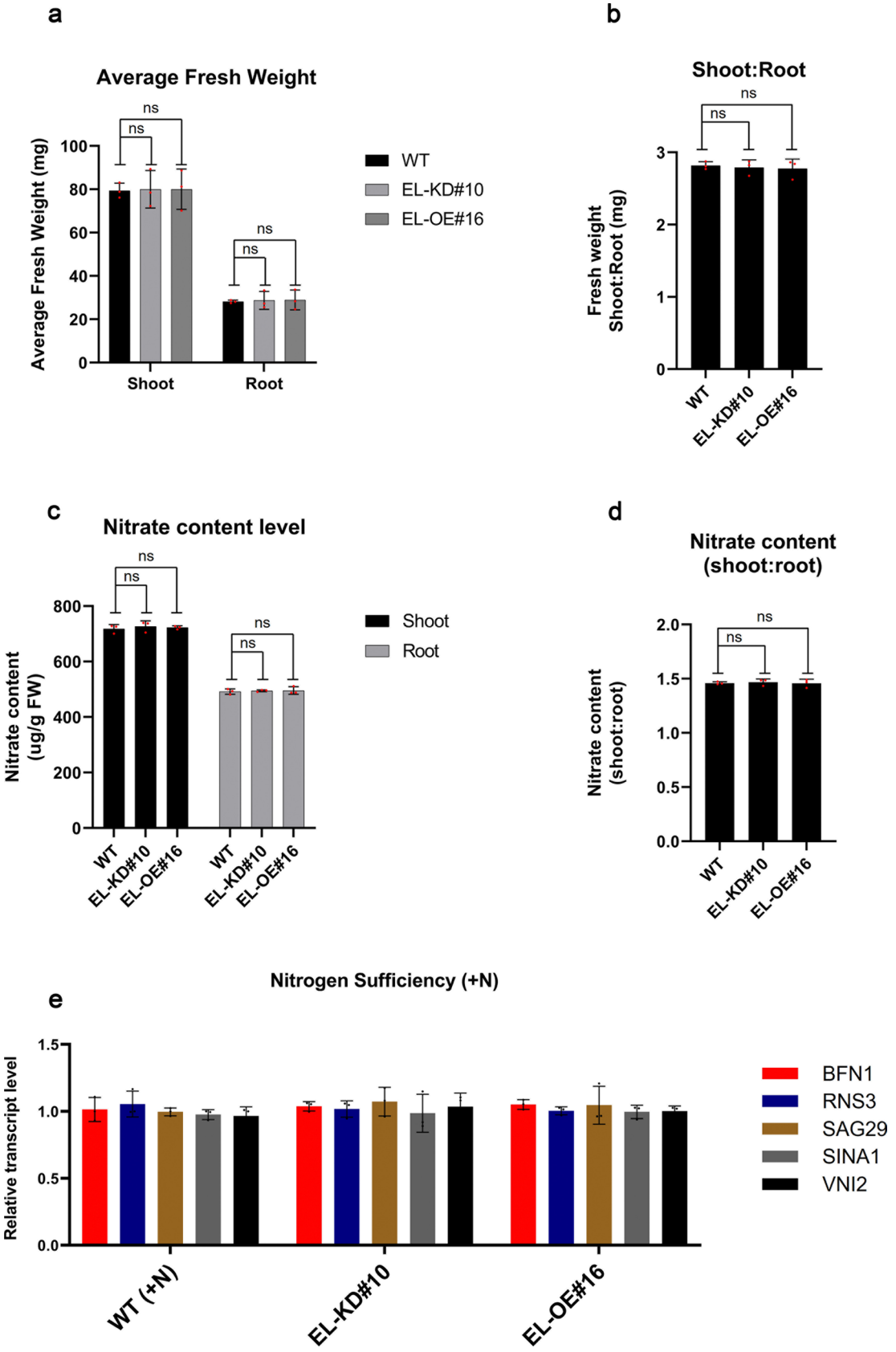

Extended Data Fig. 2 | See next page for caption.

https://doi.org/10.1038/s41477-023-01521-x

Extended Data Fig. 2 | *ELENA1* does not influence growth, nitrate content and expression of ORE1 target genes under nitrogen sufficient (+N) conditions. (a) Average fresh weight of shoots and roots in the indicated genotypes grown under +N conditions. (b) Shoot-to-root ratio of fresh weight in the indicated genotypes. (c) Total nitrate content in shoots and roots of the indicated genotypes grown under +N conditions. (d) Shoot-to-root ratio of total nitrate content in the indicated genotypes. (e) Transcript analysis of *ORE1* target genes *BFN1*, *RNS3*, *SAG29*, *SINA1* and *VNI2* in the indicated genotypes treated on +N medium. ns indicated not statistically significant, $P > 0.05$; two-way ANOVA, multiple comparison with Dunnett post hoc analysis. Value of each gene in WT (+ N) was set to 1. (a, b, c, d, e) Data are means ± SD. n = 3 and individual data points as overlays. ns, no statistical difference; one-way ANOVA (a,b,c,d), two-way anova (e) Dunnett's multiple comparison analysis.

https://doi.org/10.1038/s41477-023-01521-x

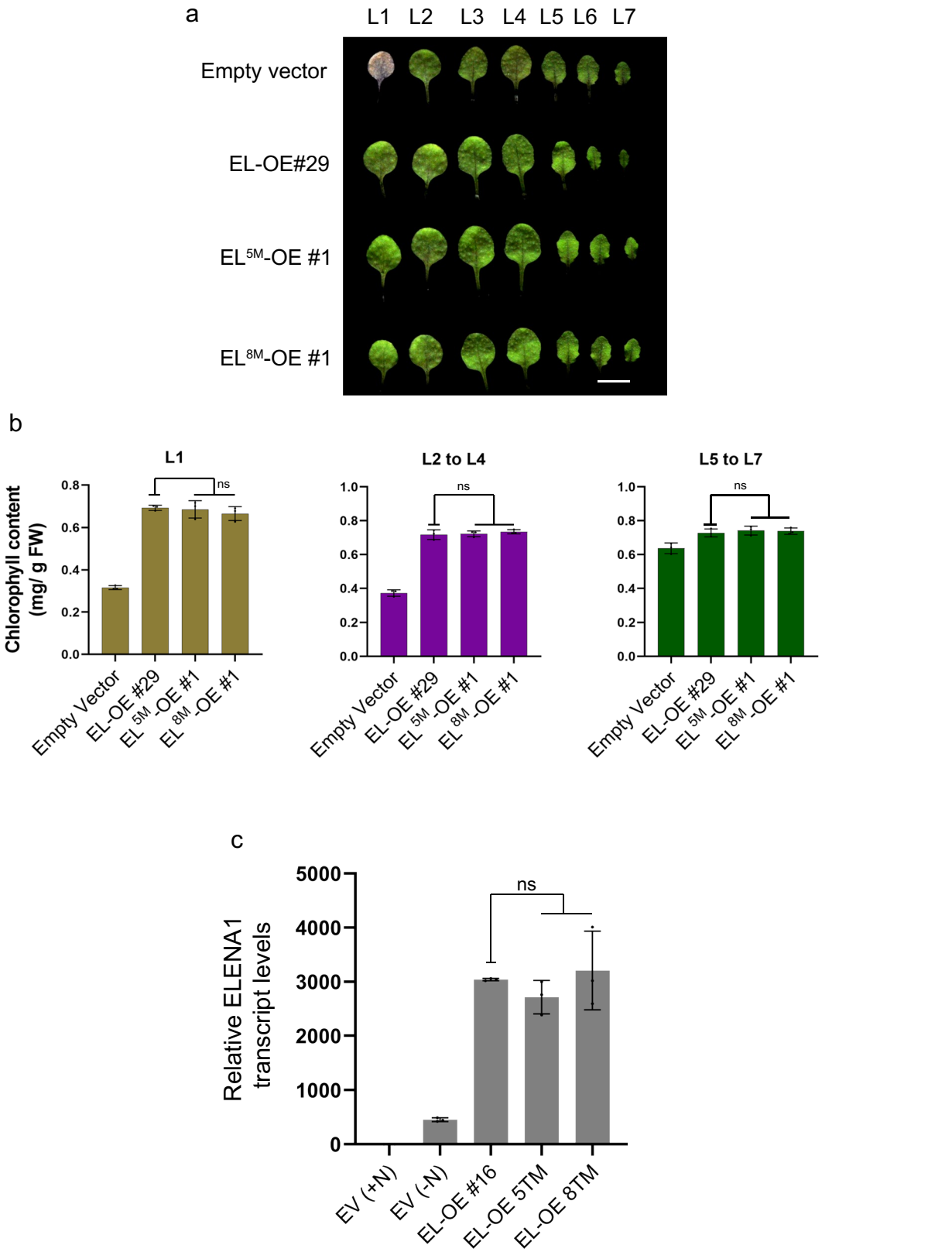

Extended Data Fig. 3 | *ELENA1* transcripts are bona fide lncRNAs under nitrogen deficiency (-N). (a) -N induced leaf senescence phenotype of empty vector transgenic plant, *EL-OE#29*, *EL^{5M}-OE #1* and *EL^{8M}-OE #1*. Scale bar represents 1 cm. (b) Total chlorophyll content in different leaf groups of the indicated genotypes treated on -N medium. Leaf number, L. FW, fresh weight. (c) Expression level of *ELENA1* in the indicated genotypes treated on -N medium. Value of EV (+ N) was set to 1. (b, c) Data are means ± SD. n = 3 (biologically independent samples). Each sample contained 20 seedlings and individual data points as overlays. ns, no statistical difference; one-way ANOVA, Dunnett's multiple comparison analysis.

https://doi.org/10.1038/s41477-023-01521-x

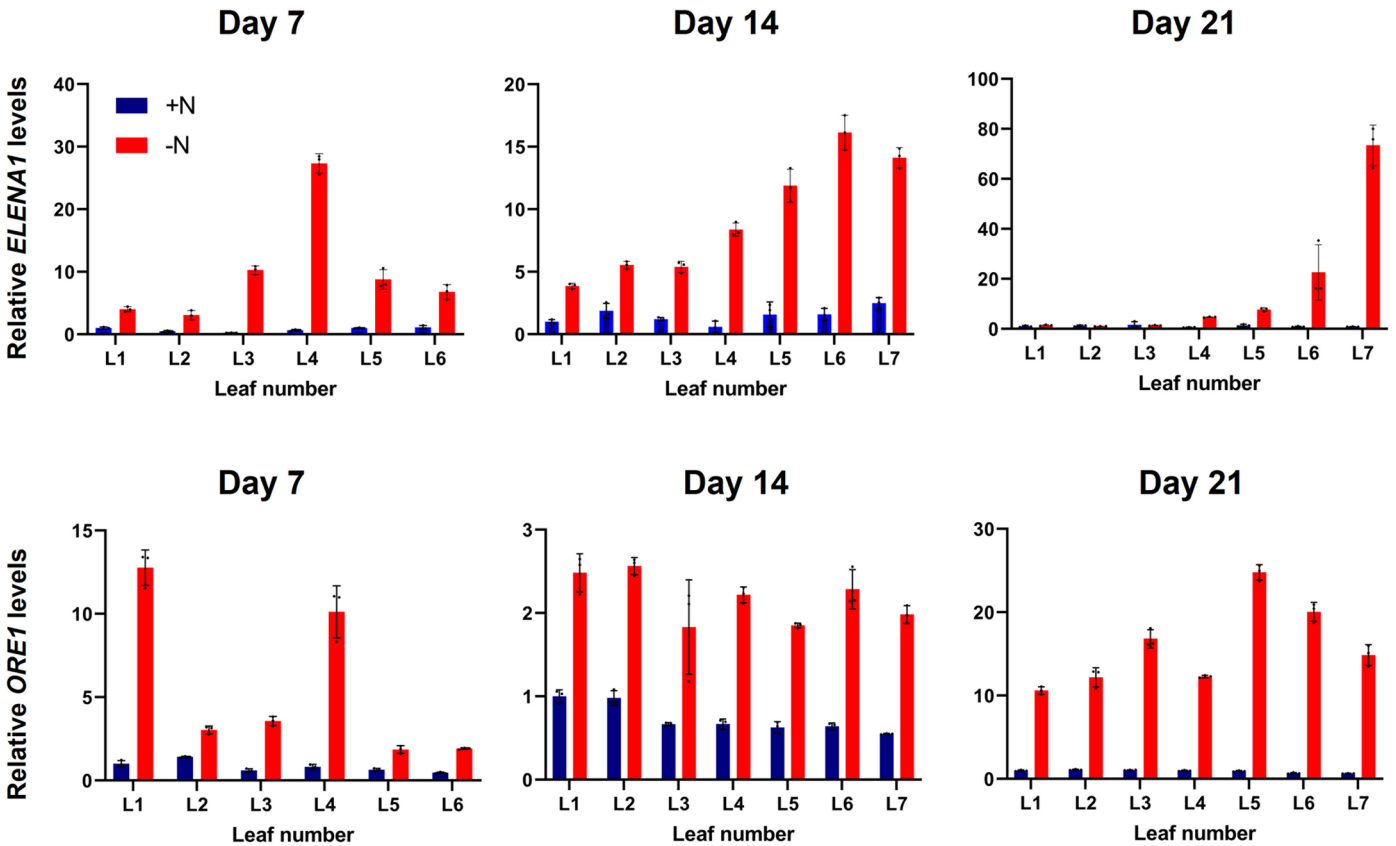

Extended Data Fig. 4 | Time course analysis of *ELENA1* and *ORE1* transcripts in individual leaf during nitrogen deficiency (-N) in WT plants. RT-qPCR analysis of *ELENA1* and *ORE1* transcripts in various leaves of WT plants Data are means ± SD. n = 3 (biologically independent samples) and individual data points as overlays. The expression level of L1 + N at each indicated day was set at 1.

https://doi.org/10.1038/s41477-023-01521-x

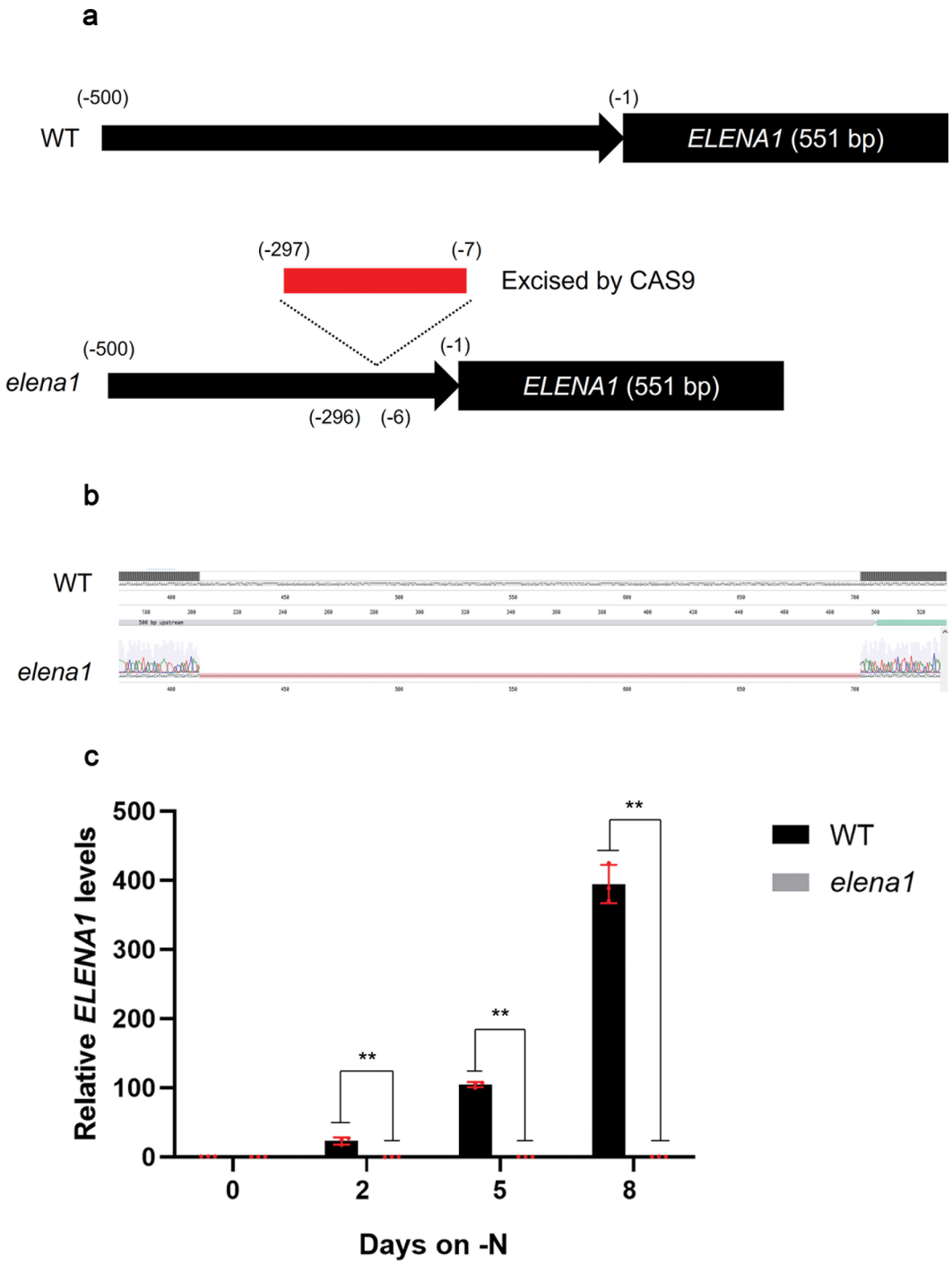

Extended Data Fig. 5 | Genetic information of *elena1* mutant. (a) Schematic of *ELENA1* genomic loci in WT and *elena1*. In *elena1*, the genomic region between -297 and -7 upstream of transcriptional start site of *ELENA1* was excised by CAS9. (b) DNA sequencing result of indicated genomic loci in (A) of *elena1* aligned to that of WT. (c) *ELENA1* expression level of WT and *elena1* treated on nitrogen deficient (-N) medium. Data are means ± SD. n = 3 (biologically independent samples). Each sample contained 20 seedlings and individual data points as overlays. Expression level in day 0 WT was set as 1. Asterisks indicate statistically significant difference compared with WT. $^{**}P < 0.01$; one-way ANOVA, Dunnett's multiple comparison analysis.

https://doi.org/10.1038/s41477-023-01521-x

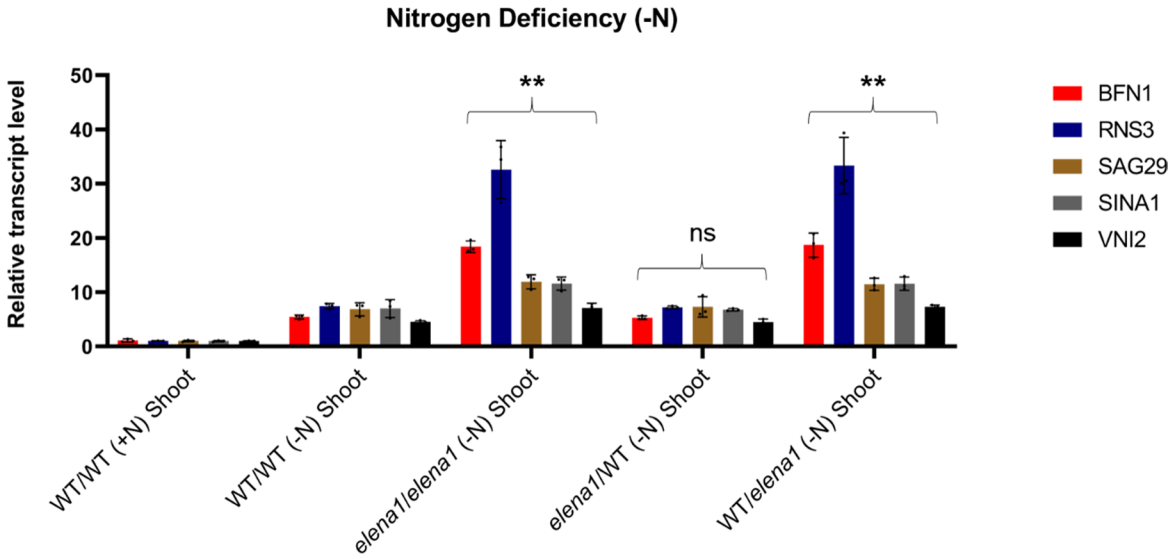

Extended Data Fig. 6 | Transcript analysis of ORE1 target genes in shoots of graft chimeras under -N. RT-qPCR analysis of *ORE1* target genes *BFN1*, *RNS3*, *SAG29*, *SINA1* and *VNI2* in the indicated genotypes treated on +N or -N medium. Data are means ± SD. n = 3 (biologically independent samples). Value of each gene transcript in WT (+ N) was set to 1. Each sample contained 20 seedlings and individual data points as overlays. Asterisks indicate statistically significant difference compared with WT/WT (+ N). ns, no statistical difference.**$P < 0.01$; two-way ANOVA, Dunnett's multiple comparison analysis.

https://doi.org/10.1038/s41477-023-01521-x

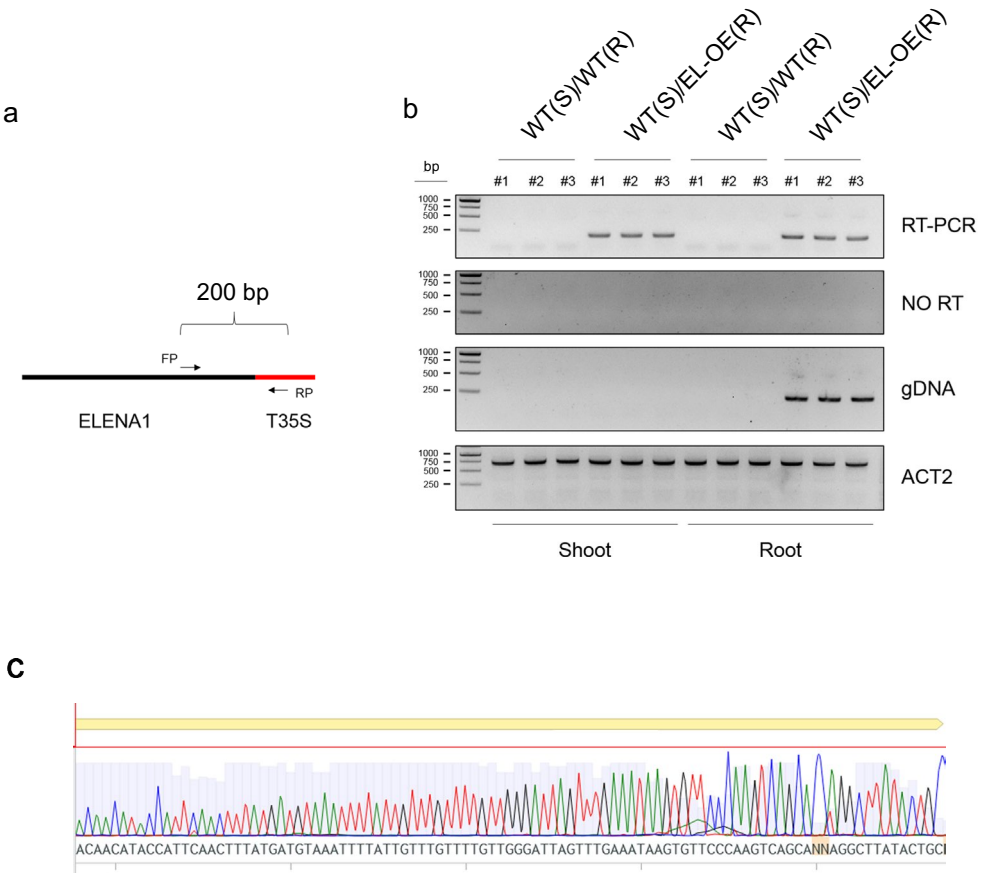

Extended Data Fig. 7 | Transgenic *ELENA1* transcripts are root-to-shoot mobile under nitrogen deficient (-N) condition. (a) Schematic of primer design for specific detection of transgenic *ELENA1*. (b) *ELENA1* transcripts root-to-shoot mobility assay. Indicated graft chimeras were generated and treated on -N. Shoot and root RNA and gDNA of the graft chimeras were analysed by RT-PCR, no RT PCR, gDNA-PCR and ACT2 correspondingly for 35x PCR cycles. Numbers indicate biological repeat sample. (c) DNA sequencing of the PCR amplicon in RT-PCR reaction in (b).

https://doi.org/10.1038/s41477-023-01521-x

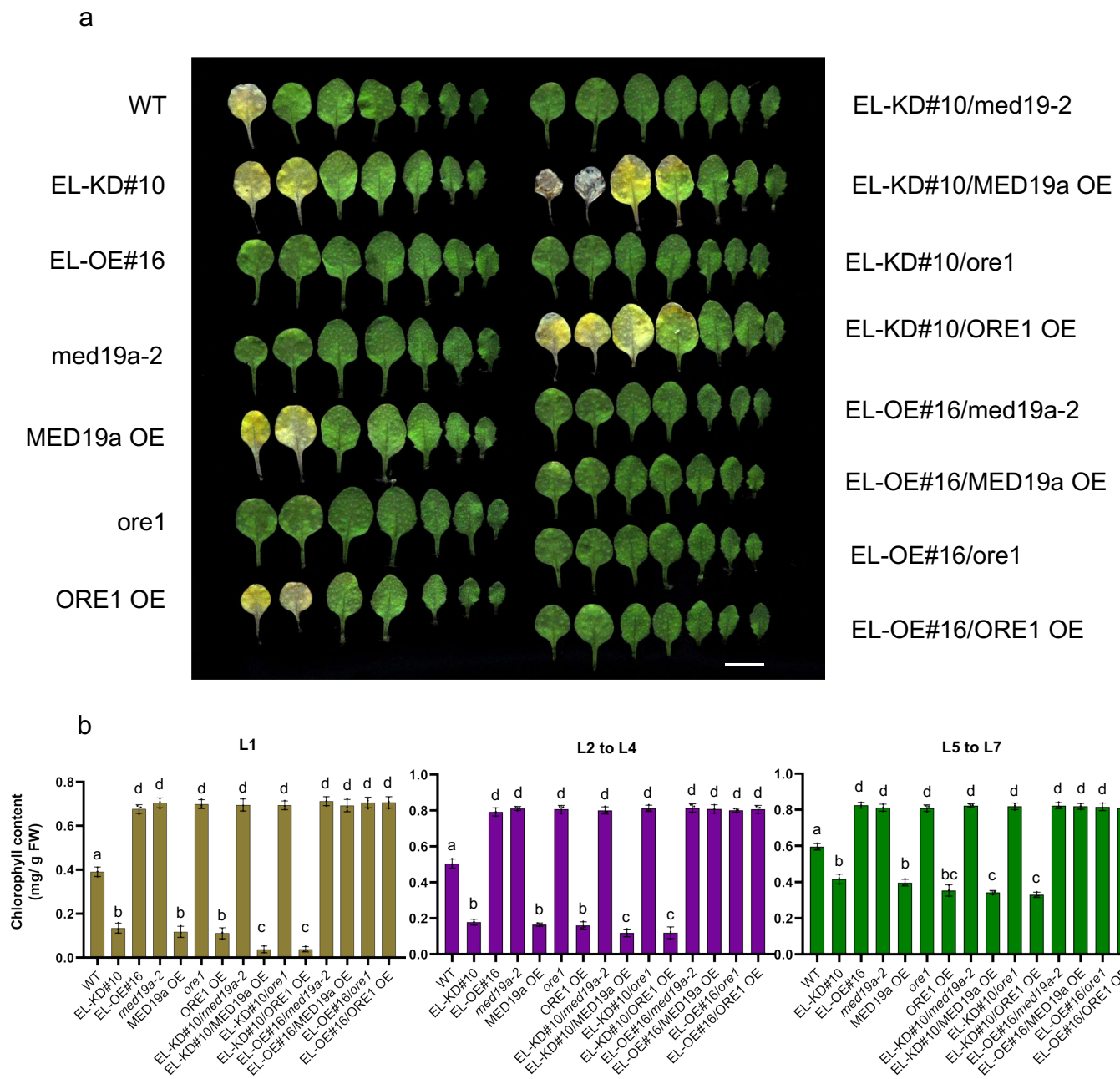

Extended Data Fig. 8 | Comprehensive genetic analysis of MED19a/ORE1/*ELENA1* under nitrogen deficient (-N) condition. (a)-N induced leaf senescence phenotype of the indicated genotypes. Scale bar represents 1 cm. (b) Total chlorophyll content in different leaf groups of the indicated genotypes treated on -N medium. Leaf number, L. FW, fresh weight. Data are means ± SD. n = 3 (biologically independent samples). Each sample contained 20 seedlings and individual data points as overlays. Alphabets indicate statistically significant groups with $P < 0.05$. One-way ANOVA, Tukey's multiple comparison analysis.

https://doi.org/10.1038/s41477-023-01521-x

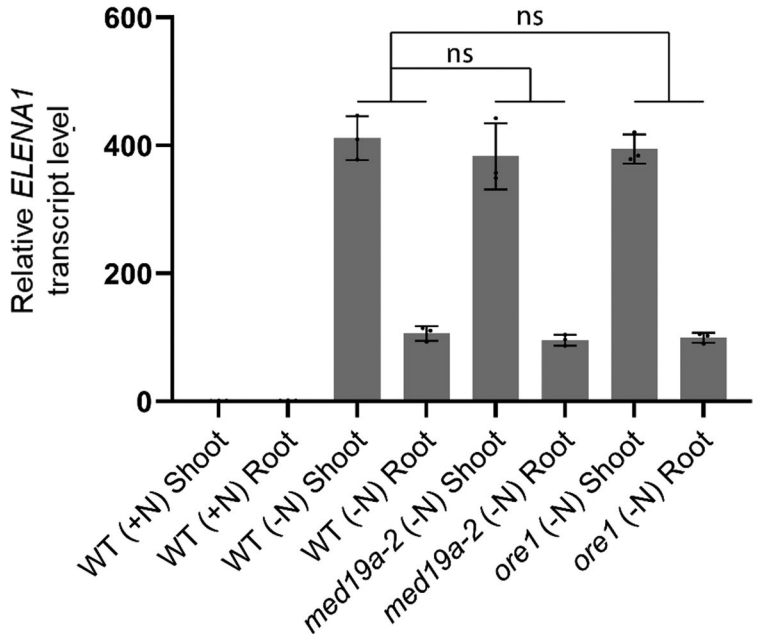

Extended Data Fig. 9 | *ELENA1* transcripts show systemic root-to-shoot movement under nitrogen deficiency (-N) is independent of MED19a and ORE1. *ELENA1* expression levels in shoots and roots of WT (+ N), WT (-N), *med19a-2* (-N), and *ore1* (-N). Data are means ± SD. n = 3 (biologically independent samples). Value of WT (+ N) shoot was set to 1. Each sample contained 20 seedlings and individual data points were shown. ns, no statistical difference; one-way ANOVA, Dunnett's multiple comparison analysis.

https://doi.org/10.1038/s41477-023-01521-x

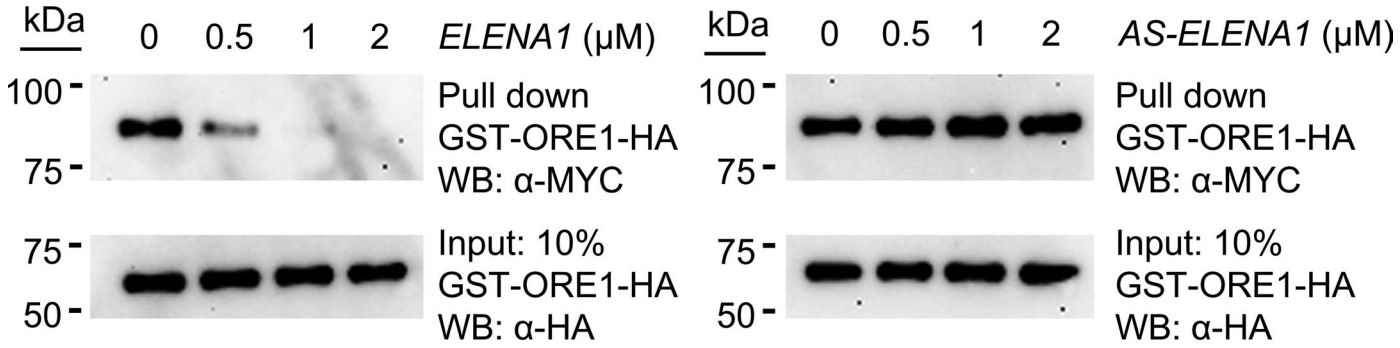

Extended Data Fig. 10 | Effects of increasing concentrations of *ELENA1* and antisense *ELENA1* transcripts on MED19a-ORE1 complex *in vitro*. Left panel, sense *ELENA1* RNA; Right panel, antisense *ELENA1* RNA. Experiment was repeated 3 times with similar results.

nature portfolio

Corresponding author(s): Nam-Hai Chua

Last updated by author(s): 25-7-2023

Reporting Summary

Nature Portfolio wishes to improve the reproducibility of the work that we publish. This form provides structure for consistency and transparency in reporting. For further information on Nature Portfolio policies, see our Editorial Policies and the Editorial Policy Checklist.

Statistics

For all statistical analyses, confirm that the following items are present in the figure legend, table legend, main text, or Methods section.

n/a	Confirmed	
☐	☒	The exact sample size (*n*) for each experimental group/condition, given as a discrete number and unit of measurement
☐	☒	A statement on whether measurements were taken from distinct samples or whether the same sample was measured repeatedly
☐	☒	The statistical test(s) used AND whether they are one- or two-sided *Only common tests should be described solely by name; describe more complex techniques in the Methods section.*
☒	☐	A description of all covariates tested
☐	☒	A description of any assumptions or corrections, such as tests of normality and adjustment for multiple comparisons
☐	☒	A full description of the statistical parameters including central tendency (e.g. means) or other basic estimates (e.g. regression coefficient) AND variation (e.g. standard deviation) or associated estimates of uncertainty (e.g. confidence intervals)
☐	☒	For null hypothesis testing, the test statistic (e.g. *F*, *t*, *r*) with confidence intervals, effect sizes, degrees of freedom and *P* value noted *Give P values as exact values whenever suitable.*
☐	☒	For Bayesian analysis, information on the choice of priors and Markov chain Monte Carlo settings
☒	☐	For hierarchical and complex designs, identification of the appropriate level for tests and full reporting of outcomes
☒	☐	Estimates of effect sizes (e.g. Cohen's *d*, Pearson's *r*), indicating how they were calculated

Our web collection on statistics for biologists contains articles on many of the points above.

Software and code

Policy information about availability of computer code

Data collection	1) For qPCR, Biorad CFX96 was used. 2) For western blot, iBright Thermo Fisher Scientific was used. 3) For chlorophyll and nitrate content, Tecan plate reader was used. 4) For confocal microscope imaging, SP8 (Leica) or FV3000 (Olympus) was used.
Data analysis	1) GraphPad Prism Version 9 was used for statistical analysis 2) ImageJ Version 1.53t for image processing

For manuscripts utilizing custom algorithms or software that are central to the research but not yet described in published literature, software must be made available to editors and reviewers. We strongly encourage code deposition in a community repository (e.g. GitHub). See the Nature Portfolio guidelines for submitting code & software for further information.

Data

Policy information about availability of data

All manuscripts must include a data availability statement. This statement should provide the following information, where applicable:

- Accession codes, unique identifiers, or web links for publicly available datasets
- A description of any restrictions on data availability
- For clinical datasets or third party data, please ensure that the statement adheres to our policy

All data generated or analysed in this study are included in this article and Supplementary Information files. The materials and transgenic plants generated in this current study are available from the corresponding author on reasonable request.

Human research participants

Policy information about studies involving human research participants and Sex and Gender in Research.

Reporting on sex and gender	N.A
Population characteristics	N.A
Recruitment	N.A
Ethics oversight	N.A

Note that full information on the approval of the study protocol must also be provided in the manuscript.

Field-specific reporting

Please select the one below that is the best fit for your research. If you are not sure, read the appropriate sections before making your selection.

☒ Life sciences ☐ Behavioural & social sciences ☐ Ecological, evolutionary & environmental sciences

For a reference copy of the document with all sections, see nature.com/documents/nr-reporting-summary-flat.pdf

Life sciences study design

All studies must disclose on these points even when the disclosure is negative.

Sample size	Sample sizes are reported. No sample size calculation was performed. Sample sizes were chosen by the reproducibility of results.
Data exclusions	No data point was excluded
Replication	Results from three independent biological repeats were reported and the attempts were successful consecutively.
Randomization	Transgenic plants are randomly selected from a pool of transformants to minimize position effect. Further randomization is not relevant for this study.
Blinding	Author who performed the experiment also analysed the data. Hence blind is not applied.

Reporting for specific materials, systems and methods

We require information from authors about some types of materials, experimental systems and methods used in many studies. Here, indicate whether each material, system or method listed is relevant to your study. If you are not sure if a list item applies to your research, read the appropriate section before selecting a response.

Materials & experimental systems

n/a	Involved in the study
☐	☒ Antibodies
☒	☐ Eukaryotic cell lines
☒	☐ Palaeontology and archaeology
☒	☐ Animals and other organisms
☒	☐ Clinical data
☒	☐ Dual use research of concern

Methods

n/a	Involved in the study
☒	☐ ChIP-seq
☒	☐ Flow cytometry
☒	☐ MRI-based neuroimaging

Antibodies

Antibodies used: MYC tag antibody (16286-1-AP), HA tag antibody (51064-2-AP), DYKDDDDK Tag (9A3) Mouse mAb

Validation: Antibodies were used based on manufacturers' instruction and specificity validations were performed by using WT, transgenic plants, and recombinant proteins.